Published in final edited form as:

*Circ Res*. 2017 April 14; 120(8): 1318–1325. doi:10.1161/CIRCRESAHA.116.310277.

# Myocardial Tissue Engineering With Cells Derived from Human Induced-Pluripotent Stem Cells and a Native-Like, High-Resolution, 3-Dimensionally Printed Scaffold

**Ling Gao**[1], **Molly E. Kupfer**[2], **Jangwook P. Jung**[2], **Libang Yang**[2], **Patrick Zhang**[2], **Yong Da Sie**[3], **Quyen Tran**[3], **Visar Ajeti**[3], **Brian T. Freeman**[2], **Vladimir G. Fast**[1], **Paul J. Campagnola**[3], **Brenda M. Ogle**[2,*], and **Jianyi Zhang**[1,*]

[1]Department of Biomedical Engineering, School of Medicine, School of Engineering, University of Alabama at Birmingham

[2]Department of Biomedical Engineering, University of Minnesota – Twin Cities

[3]Department of Biomedical Engineering, University of Wisconsin – Madison, Madison

## Abstract

**Rationale—**Conventional three-dimensional (3D) printing techniques cannot produce structures of the size at which individual cells interact.

**Objective—**Here, we used multiphoton-excited, 3-dimensional printing (MPE-3DP) to generate a native-like, extracellular matrix (ECM) scaffold with submicron resolution, and then seeded the scaffold with cardiomyocytes (CMs), smooth-muscle cells (SMCs), and endothelial cells (ECs) that had been differentiated from human induced-pluripotent stem cells (iPSCs) to generate a human, iPSC-derived cardiac muscle patch (hCMP), which was subsequently evaluated in a murine model of myocardial infarction (MI).

**Methods and Results—**The scaffold was seeded with ~50,000 human, iPSC-derived CMs, SMCs, and ECs (in a 2:1:1 ratio) to generate the hCMP, which began generating calcium transients and beating synchronously within 1 day of seeding; the speeds of contraction and relaxation and the peak amplitudes of the calcium transients increased significantly over the next 7 days. When tested in mice with surgically induced MI, measurements of cardiac function, infarct size, apoptosis, both vascular and arteriole density, and cell proliferation at week 4 after treatment were significantly better in animals treated with the hCMPs than in animals treated with cell-free scaffolds, and the rate of cell engraftment in hCMP-treated animals was 24.5% at week 1 and 11.2% at week 4.

Addresses correspondence to: Dr. Jianyi Zhang, Department of Biomedical Engineering, University of Alabama at Birmingham, jayzhang@uab.edu. Dr. Brenda M. Ogle, Department of Biomedical Engineering, University of Minnesota – Twin Cities, ogle@umn.edu.
B.M.O. and J.Z. are both corresponding authors.

**DISCLOSURES**
None.

**Conclusions—**Thus, the novel MPE-3DP technique produces ECM-based scaffolds with exceptional resolution and fidelity, and hCMPs fabricated with these scaffolds may significantly improve recovery from ischemic myocardial injury.

### Keywords

Heart; myocardial infarction; tissue engineering

### Subject Terms

Myocardial Infarction; Cell Therapy; Stem Cells

## INTRODUCTION

Although recent large-animal studies have shown that recovery from myocardial injury can be improved by injecting cardiac cells that have been differentiated from human induced-pluripotent stem cells (hiPSCs), the structural support and synchronized contractile activity of a transplanted myocardial tissue equivalent (MTE) could provide additional benefits. Tissue engineers are beginning to improve the effectiveness of MTE engineering for regenerative myocardial therapies[1–3] by developing techniques that can enhance the engraftment, improve the MTE maturation[4, 5] and long-term functional benefits.[6, 7] These efforts may be aided by incorporating some of the more complex features of the myocardial extracellular matrix (ECM) into the tissue's design. This level of complexity cannot be reproducibly achieved with established manufacturing technologies, but a newer modality, 3D printing, has been successfully used to build structures with defined geometries from heterogeneous materials[8] and, consequently, may be used for generating scaffolds that mimic the ECM of native cardiovascular tissues. However, key structural features of the native ECM need to be identified and incorporated (with adequate resolution and reliability) into a scaffold to promote cell function and limit detrimental effects. In addition, from the potential clinical application perspective, a high level of quality control of the scaffold product is required, which can only be achieved by a computer controlled 3D printing technology.

The position of crosslinks within a matrix of photoactive biological polymers can be controlled with high resolution. Printers that utilize single-photon excitation coupled to a sequence of photomasks can achieve approximately 30 micron resolution in x, y and approximately 50 micron resolution in z. A more advanced technique, multiphoton excited (MPE) photochemistry, can restrict excitation (and, consequently, the photochemical reaction) in three dimensions via a method that is analogous to multi-photon laser scanning microscopy (MPLSM).[9–14] Notably, the resolution of the features (<1 μm) is determined by the MPE point spread function and can therefore approximate the feature size of components of the extracellular matrix.[15] The technique can also be combined with rapid prototyping and computer-aided design[16] to fabricate essentially any 3D structure that can be drawn.

For the experiments described in this report, we used our novel technique, multiphoton-excited three-dimensional printing (MPE-3DP), to generate a scaffold with a native-like

cardiac ECM architecture from a solution of a photoactive gelatin polymer and then seeded the scaffold with cardiac cells (cardiomyocytes [CMs], endothelial cells [ECs], and smooth muscle cells [SMCs]) that had been differentiated from human, cardiac-lineage, induced-pluripotent stem cells (hciPSCs)[17] to generate an hciPSC-derived cardiac muscle patch (hCMP). The hCMP was subsequently characterized via a series of *in vitro* analyses and then tested in a murine model of ischemic myocardial injury.

## METHODS

A detailed description of the experimental procedures used in this investigation is provided in the online Data Supplement.

## RESULTS

### Fabrication of an ECM scaffold based on templates derived from optical image stacks of murine myocardium

Our approach can be summarized in two steps: first, native, murine, adult myocardial tissue was examined to determine the size and distribution of various ECM features, which were incorporated into a 3D template; then, the template was scanned and used to map the positions of crosslinks in a solution of a photoactive polymer (Figure 1A). Importantly, our scanning technique, modulated raster scanning, maps the template directly to the scaffold by monitoring the brightness of each point in the image, and it is accurate to resolutions of less than 1 μm. To our knowledge, this is the first time modulated raster scanning has ever been successfully used to control the fabrication of a tissue-engineered scaffold and, consequently, our results are particularly relevant for applications that require the fibrillar and mesh-like structures present in cardiac tissue.[18]

We chose to base our template on the distribution of fibronectin in murine myocardium (Figure 1B and 1C). Fibronectin is uniformly distributed around each CM, so it can be used to determine the dimensions of each individual cell compartment to form a grid (here termed, Adult Simulate). The scaffold was generated from a solution of gelatin methacrylate, which can be crosslinked into complex structures with high efficiency, allows creation of complex structures with thickness of approximately 100 μm (Online Video I, II and III), is biologically inert when both crosslinked and degraded, and the denatured collagen exposes cell binding sites (including Arg-Gly-Asp, RGD), which should readily adhere to the seeded cells and support biochemical signaling via focal adhesions.[19] Analysis of the native myocardium suggested that CMs reside in channels that are approximately 15 μm by 100 μm which, when incorporated in the hCMP scaffold (Figure 1D and 1E), yielded a robust structure with high reproducibility and exceptional fidelity in both coverage area (≥95%) and intensity variation (≥85%).

### Integration of hciPSC-derived cardiac cells in hCMPs

The hciPSCs were reprogrammed from human cardiac fibroblasts and differentiated into hciPSC-CMs, hciPSC-SMCs, and hciPSC-ECs; then, the differentiated cells were characterized via the expression of lineage-specific markers (Online Figure I), and the hCMP was formed by seeding ~50,000 cells (in a 2:1:1 ratio of hciPSC-CMs, hciPSC-

SMCs, and hciPSC-ECs, respectively) into the fabricated scaffold, where they quickly became assimilated and occupied most of the free space (Figure 1D). The hciPSC-CMs began generating calcium transients (Figure 2A) and beat synchronously across the entire hCMP within one day of seeding (Online Video IV and V). Over the next seven days, the speeds of contraction and relaxation, the peak amplitude of the calcium transients (Figure 2B and 2C), and the expression of several genes required for contractile function (cTnT, cTnI, and αMHC) and for generating calcium transients (SERCA2α, RYR2, CASQ2) increased significantly (Online Figure II). Contractile and calcium-transient gene expression was also greater in the hCMPs than in monolayers grown from equivalent populations of hiPSC-derived cardiac cells on day 7. Optical mapping of transmembrane potentials (Figure 2D and 2E) revealed macroscopically continuous action potential propagation in hCMPs, showing an excellent functional electrophysiological communications between cells. Conduction velocity in hCMPs increased linearly with the increase of pacing cycle length (CL), reaching 18.8±0.8 cm/s at 800 ms pacing CL (Figure 2F). Action potential durations, $APD_{50}$ and $APD_{80}$, were about 214±10.4 and 270±12.7 ms at 800 ms pacing CL, separately, and also showed significant correlation with pacing rate (Figure 2G). Autofluorescence images obtained via 2-photon microscopy on day 7 (Figure 2H) indicated that the cells had aligned with the channels of the fabricated scaffold (Figure 2I) to form multinucleate cells with an aspect ratio (i.e., cell length:width) of approximately 5.5:1 (Figure 2J), which is close to the characteristic ratio observed in native CMs (7:1). Analysis of hCMPs stained for expression of the CM protein cTnI, α-smooth muscle actin (αSMA), and the endothelial marker CD31 (Figure 2K) indicated that the original 2:1:1 ratio of hciPSC-CMs, -SMCs, and -ECs was largely retained (Figure 2L), with CMs comprising ~45% of the remaining cells. The 7-day survival rate of hciPSC-CMs in the hCMP was similar to that observed when cells were maintained on Matrigel-coated plates and significantly greater than the rate achieved by culturing the cells with bovine pericardium or polyethylene glycol (Figure 2M).

## In vivo evaluations of hCMP transplantation in a murine model of myocardial infarction

*In vivo* assessments of the hCMPs were performed in a murine model of myocardial infarction (MI). MI was surgically induced as described previously,[20] then, animals in the MI+hCMP group were treated with two hCMPs, animals in the MI+Scaffold group were treated with two patches of scaffold material without cells, and animals in the MI group received neither the hCMP nor the cell-free scaffold. The hCMPs and scaffolds were positioned over the site of infarction (Figure 3A) and held in place by covering them with a piece of decellularized bovine pericardium that was sutured to the heart to avoid movement of hCMPs off the heart. The decellularized bovine pericardium above the hCMP has beneficial effect of preventing the adhesion between the heart/hCMP and the chest. The Sham group underwent all surgical procedures for MI induction except the ligation step and recovered without either experimental treatment. Quantitative PCR measurements for expression of the human Y chromosome indicated that 24.5±2.6% of the transplanted cells remained engrafted in the hearts of MI+hCMP animals for at least one week after transplantation (Figure 3B). By week 4, the engraftment rate had declined to 11.2±2.3%, which is still much higher than the rate reported in previous studies of cell-based myocardial therapy.[21, 22] In order to assess the engraftment rate by counting the grafted human cells as evidenced by human-specific nuclear antigen (HNA) positivity, we also used histologic

assessment of consecutive sections of the heart that spans the entire area covered by the engrafted patch, and counting the grafted human cells as evidenced by HNA positivity.[17, 23] The engraftment rate of the 7 hearts studied using the histology method is 13.6 ± 2.2%, which is in agreement with the quantitative PCR (11.2 ± 2.3%). The ratio of the hciPSC-tri lineage cardiac cells at week 1 and 4 was also examined. The engrafted hciPSC-CMs were identified by the expression of both green fluorescent protein (GFP) and cTnI, engrafted hiPSC-ECs were identified by expression of human specific CD31 (hCD31), and engrafted hiPSC-SMCs were identified by the expression of both GFP and αSMA. At week 1 post transplantation the ratio of hciPSC-CMs, hciPSC-SMCs, and hciPSC-ECs was 1.42: 0.93: 1; at week 4 the ratio was 0.67: 0.86: 1 for hciPSC-CMs, hciPSC-SMCs, and hciPSC-ECs, respectively. Hematoxylin and Eosin (HE) staining (Figure 3C), and immunofluorescence analysis of HNA, GFP, cTnI, αSMA, and hCD31 expression (Figure 3C and 3D) showed evidence of all three transplanted cell lineages in the treated region

Cardiac function was evaluated on day 28 after injury via echocardiographic assessments (Figure 4A) of left-ventricular ejection fraction and fractional shortening; both parameters were significantly greater for animals in the MI+hCMP group than in MI+Scaffold or MI animals (Figure 4B and 4C), while measurements in the MI+Scaffold and MI groups were similar. Infarcts were also significantly smaller, while the thickness of the infarcted region of the myocardial wall was significantly greater, in MI+hCMP hearts than in MI or MI +Scaffold hearts (Figure 4D–4F), and analyses of TUNEL-stained sections (Online Figure IIIA and IIIB) and sections stained for the presence of CD31 and αSMA (Online Figure IIIC–IIIE) indicated that apoptotic cells were significantly less common, while vascular structures (including arterioles) were significantly more common, at the border of the infarcted region in hCMP-treated animals than in the corresponding regions of hearts from animals in the MI+Scaffold or MI groups. hCMP treatment was also associated with significant increases in the number of cells that expressed the proliferation marker Ki67 (Online Figure IV). Thus, the transplanted hCMPs appeared to improve recovery from myocardial injury by, at least in part, reducing apoptosis, promoting angiogenesis, and increasing cell proliferation.

## DISCUSSION

The fate specification of progenitor cells in the developing heart is critically dependent on the spatial and temporal factors of the ECM where the progenitor cells reside. In human pluripotent stem cell differentiation to endothelial cells, the rate and quality of derived endothelial cells are critically influenced by the temporal factors in 3D ECM. [24] The myocardial ECM provides substrates for cell adhesion, sequesters soluble factors, and serves as a conduit for mechanical signaling. Our recent efforts to characterize the ECM of the developing heart have provided us with an extensive body of knowledge regarding the nanoscale distribution of the ECM,[25] and by combining this knowledge with MPE-3DP, we were able to generate a scaffold that is structurally native-like.[16] The technique couples MPE with modulated raster scanning to induce crosslinks in a solution of a photoactive gelatin polymer, thereby creating an ECM scaffold with exceptionally high resolution. Notably, construction was guided by a template composed of features that had been identified in the ECM of a native adult murine heart, which suggests that the technique may

be able to replicate the unique architecture of the myocardial ECM in each individual. Furthermore, when hCMPs were generated by seeding the scaffolds with hciPSC-derived cardiac cells and transplanted into infarcted mouse hearts, the treatment was associated with significant improvements in cardiac function, infarct size, apoptosis, vascular density, and cell proliferation. Thus, the hCMPs produced for this report may represent an important step toward the clinical use of 3D-printing technology.

Our novel technique is the first to achieve a resolution of 1 μm or less and, consequently, can reliably control the thickness of the walls that separate adjacent channels. Channel-wall thickness may be a particularly important parameter for myocardial tissues, because contractions in adjacent fibers must be synchronized by signaling mechanisms that traverse the wall. Notably, the seeded cells quickly settled into the engineered channels of the scaffolds generated for this report, and synchronized beating was observed as early as one day after cell seeding, which suggests that individual cells interacted with the features of the scaffold, and that inter-channel coupling mechanisms were quickly established.

The functional improvement associated with hCMP transplantation in the murine MI model suggests that this goal may have been at least partially achieved. Thus, in future investigations we will use optical mapping technology to determine whether transplanted hCMPs are electromechanically coupled to native myocardial tissues.[26]

In conclusion, we have developed a method by which the principles of 3D printing and photochemistry can be combined to generate an ECM scaffold with unprecedented resolution from a template based on the architecture of native myocardial ECM. When hCMPs were generated by seeding the scaffolds with hciPSC-derived cardiac cells, the scaffold promoted cell viability and electromechanical coupling *in vitro*, and the hCMPs were associated with high levels of cell engraftment, as well as significant improvements in cardiac function, infarct size, apoptosis, vascularity, and cell proliferation in a murine MI model. Subsequent investigations will focus on methods for creating hCMPs of sufficient size for large-animal studies and means to improve effectiveness of the hCMPs by incorporating mixtures of ECM proteins into the scaffold.

## Supplementary Material

Refer to Web version on PubMed Central for supplementary material.

## Acknowledgments

**SOURCES OF FUNDING**

This work was supported by the following funding sources: National Science Foundation, Award CBET-1445650; Lillehei Heart Institute, UMN, High Risk High Reward; Institute for Engineering and Medicine, UMN, Pilot Grant, and NIH RO1 HL 99507, HL114120, HL 131017, UO1 134764.

## Nonstandard Abbreviations and Acronyms

| | |
|---|---|
| **hiPSCs** | human induced-pluripotent stem cells |
| **3D** | three-dimensional |

| | |
|---|---|
| **ECM** | myocardial extracellular matrix |
| **MPLSM** | multi-photon laser scanning microscopy |
| **MPE-3DP** | multiphoton-excited three-dimensional printing |
| **CMs** | cardiomyocytes |
| **ECs** | endothelial cells |
| **SMCs** | smooth muscle cells |
| **hCMP** | hiPSC-derived cardiac muscle patch |
| **CL** | cycle length |
| **αSMA** | α-smooth muscle actin |
| **MI** | myocardial infarction |
| **HNA** | human-specific nuclear antigen |
| **GFP** | green fluorescent protein |
| **hCD31** | human specific CD31 |
| **BP** | bovine pericardium |

## References


1. Liu J, Hu Q, Wang Z, Xu C, Wang X, Gong G, Mansoor A, Lee J, Hou M, Zeng L, Zhang JR, Jerosch-Herold M, Guo T, Bache RJ, Zhang J. Autologous stem cell transplantation for myocardial repair. Am J Physiol Heart Circ Physiol. 2004; 287:H501–11. [PubMed: 15277194]
2. Chavakis E, Koyanagi M, Dimmeler S. Enhancing the outcome of cell therapy for cardiac repair: progress from bench to bedside and back. Circulation. 2010; 121:325–35. [PubMed: 20083719]
3. Parsa H, Ronaldson K, Vunjak-Novakovic G. Bioengineering methods for myocardial regeneration. Adv Drug Deliv Rev. 2016; 96:195–202. [PubMed: 26150344]
4. Ruan JL, Tulloch NL, Razumova MV, Saiget M, Muskheli V, Pabon L, Reinecke H, Regnier M, Murry CE. Mechanical Stress Conditioning and Electrical Stimulation Promote Contractility and Force Maturation of Induced Pluripotent Stem Cell-Derived Human Cardiac Tissue. Circulation. 2016
5. Jackman CP, Carlson AL, Bursac N. Dynamic culture yields engineered myocardium with near-adult functional output. Biomaterials. 2016; 111:66–79. [PubMed: 27723557]
6. Zimmermann WH, Melnychenko I, Wasmeier G, Didie M, Naito H, Nixdorff U, Hess A, Budinsky L, Brune K, Michaelis B, Dhein S, Schwoerer A, Ehmke H, Eschenhagen T. Engineered heart tissue grafts improve systolic and diastolic function in infarcted rat hearts. Nat Med. 2006; 12:452–8. [PubMed: 16582915]
7. Riegler J, Tiburcy M, Ebert A, Tzatzalos E, Raaz U, Abilez OJ, Shen Q, Kooreman NG, Neofytou E, Chen VC, Wang M, Meyer T, Tsao PS, Connolly AJ, Couture LA, Gold JD, Zimmermann WH, Wu JC. Human Engineered Heart Muscles Engraft and Survive Long Term in a Rodent Myocardial Infarction Model. Circ Res. 2015; 117:720–30. [PubMed: 26291556]
8. Gaetani R, Feyen DA, Verhage V, Slaats R, Messina E, Christman KL, Giacomello A, Doevendans PA, Sluijter JP. Epicardial application of cardiac progenitor cells in a 3D-printed gelatin/hyaluronic acid patch preserves cardiac function after myocardial infarction. Biomaterials. 2015; 61:339–48. [PubMed: 26043062]

9. Maruo S, Nakamura O, Kawata S. Three-dimensional microfabrication with two-photon-absorbed photopolymerization. Opt Lett. 1997; 22:132–4. [PubMed: 18183126]
10. LaFratta CN, Baldacchini T, Farrer RA, Fourkas JT, Teich MC, Saleh BEA, Naughton MJ. Replication of two-photon-polymerized structures with extremely high aspect ratios and large overhangs. J Phys Chem B. 2004; 108:11256–11258.
11. Allen R, Nielson R, Wise DD, Shear JB. Catalytic three-dimensional protein architectures. Anal Chem. 2005; 77:5089–95. [PubMed: 16097743]
12. Hoffmann JC, West JL. Three-dimensional photolithographic patterning of multiple bioactive ligands in poly(ethylene glycol) hydrogels. Soft Matter. 2010; 6:5056–5063.
13. Tayalia P, Mazur E, Mooney DJ. Controlled architectural and chemotactic studies of 3D cell migration. Biomaterials. 2011; 32:2634–41. [PubMed: 21237507]
14. Wylie RG, Ahsan S, Aizawa Y, Maxwell KL, Morshead CM, Shoichet MS. Spatially controlled simultaneous patterning of multiple growth factors in three-dimensional hydrogels. Nat Mater. 2011; 10:799–806. [PubMed: 21874004]
15. Murphy SV, Atala A. 3D bioprinting of tissues and organs. Nat Biotechnol. 2014; 32:773–85. [PubMed: 25093879]
16. Cunningham LP, Veilleux MP, Campagnola PJ. Freeform multiphoton excited microfabrication for biological applications using a rapid prototyping CAD-based approach. Opt Express. 2006; 14:8613–21. [PubMed: 19529241]
17. Zhang L, Guo J, Zhang P, Xiong Q, Wu SC, Xia L, Roy SS, Tolar J, O'Connell TD, Kyba M, Liao K, Zhang J. Derivation and high engraftment of patient-specific cardiomyocyte sheet using induced pluripotent stem cells generated from adult cardiac fibroblast. Circ Heart Fail. 2015; 8:156–66. [PubMed: 25420485]
18. Ajeti V, Lien CH, Chen SJ, Su PJ, Squirrell JM, Molinarolo KH, Lyons GE, Eliceiri KW, Ogle BM, Campagnola PJ. Image-inspired 3D multiphoton excited fabrication of extracellular matrix structures by modulated raster scanning. Opt Express. 2013; 21:25346–55. [PubMed: 24150376]
19. Nichol JW, Koshy ST, Bae H, Hwang CM, Yamanlar S, Khademhosseini A. Cell-laden microengineered gelatin methacrylate hydrogels. Biomaterials. 2010; 31:5536–44. [PubMed: 20417964]
20. Nakamura Y, Yasuda T, Weisel RD, Li RK. Enhanced cell transplantation: preventing apoptosis increases cell survival and ventricular function. Am J Physiol Heart Circ Physiol. 2006; 291:H939–47. [PubMed: 16582022]
21. Nguyen PK, Riegler J, Wu JC. Stem cell imaging: from bench to bedside. Cell Stem Cell. 2014; 14:431–44. [PubMed: 24702995]
22. Xiong Q, Ye L, Zhang P, Lepley M, Swingen C, Zhang L, Kaufman DS, Zhang J. Bioenergetic and functional consequences of cellular therapy: activation of endogenous cardiovascular progenitor cells. Circ Res. 2012; 111:455–68. [PubMed: 22723295]
23. Nakamura Y, Wang X, Xu C, Asakura A, Yoshiyama M, From AH, Zhang J. Xenotransplantation of Long Term Cultured Swine Bone Marrow-Derived Mesenchymal Stem Cells. Stem Cells. 2006
24. Zhang S, Dutton JR, Su L, Zhang J, Ye L. The influence of a spatiotemporal 3D environment on endothelial cell differentiation of human induced pluripotent stem cells. Biomaterials. 2014; 35:3786–93. [PubMed: 24485793]
25. Hanson KP, Jung JP, Tran QA, Hsu SP, Iida R, Ajeti V, Campagnola PJ, Eliceiri KW, Squirrell JM, Lyons GE, Ogle BM. Spatial and temporal analysis of extracellular matrix proteins in the developing murine heart: a blueprint for regeneration. Tissue Eng Part A. 2013; 19:1132–43. [PubMed: 23273220]
26. Matiukas A, Pertsov AM, Kothari P, Cram A, Tolkacheva EG. Optical mapping of electrical heterogeneities in the heart during global ischemia. Conf Proc IEEE Eng Med Biol Soc. 2009; 2009:6321–4. [PubMed: 19964152]

## NOVELTY AND SIGNIFICANCE

**What Is Known?**

- Cellular therapy for myocardial repair has shown some benefit in preclinical and clinical settings, but limited cell retention and associated lack of robust electromechanical coupling remain the major problems.
- Greater benefits may be achieved if the transplanted cardiac cells are provided with structural support such that synchronized contractile activity of the graft can be integrated to recipient heart.
- One approach to generate a structural support is 3D printing, which has recently advanced to include the printing of biological materials such cells and extracellular matrix proteins (ECM).

**What New Information Does This Article Contribute?**

- The article describes the implementation of multiphoton-excited three-dimensional printing (MPE-3DP) to generate a scaffold with native-like cardiac ECM architecture. The scaffold can effectively harbor stem cell-derived cardiac cell types and can be handled for effective transfer to the damaged heart.
- The cell-seeded scaffold (termed human cardiac muscle patch, hCMP) beats synchronously in a culture dish prior to transplant and with extended culture time beats with increased speed and calcium handling suggesting cardiomyocyte maturation. In vivo, measurements of cardiac function and infarct size were significantly better in infarcted hearts treated with the hCMPs than in hearts treated with cell-free scaffolds.
- The mechanisms for therapeutic improvement include improved cell engraftment, increased cellular proliferation and vascular supply with decreased apoptosis.

We demonstrate multiphoton-excited, 3D printing to generate a human cardiac muscle patch (hCMP) that could be effectively populated with cardiac cell types because it mimics the structural dimensions and protein composition of the native myocardium. In a mouse model of myocardial infarction, hCMP transplantation results in higher levels of cell engraftment, cell proliferation and myocardial vascular density, which are accompanied by a significant reduction of infarct size and improvement of left ventricular function. This work pushes the technical limits of 3D printing for cardiac tissue equivalents such that cells and extracellular matrix proteins could be manufactured precisely as designed.

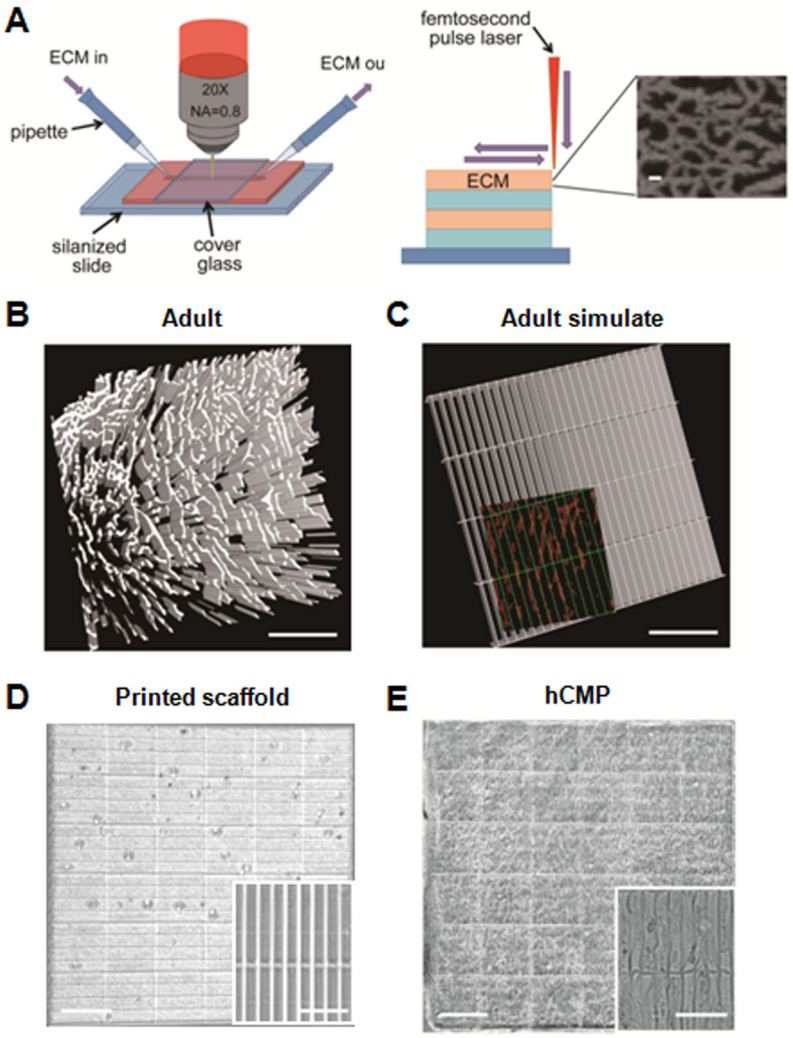


**Figure 1. hCMP fabrication via 3D-MPE**

(**A**) The ECM and associated crosslinking solution are passed through the optical interrogation path while the laser power and dwell time are modulated to deposit ECM at each x, y location in each z plane. The submicron-scale features produced in the ECM scaffold are displayed in the inset (scale bar = 1 μm). Three-dimensional structures can be generated by combining multiple layers with the same or different ECM pattern. (**B**) Sections from the heart of an adult mouse were immunofluorescently stained for the presence of fibronectin and scanned via MPE (scale bar = 200 μm); then, (**C**) the distribution of fibronectin in the native tissue was simulated in a template. The simulated channels (green, 100 μm × 15 μm) are shown overlaying the fibronectin pattern of the native tissue (red) in the inset (scale bar = 100 μm). (**D–E**) The simulated template was used to determine the position of crosslinks in a solution of gelatin methacrylate, thereby producing a native-like ECM scaffold (**D**); then, the scaffold was seeded with hiPSC-derived CMs, ECs, and SMCs to generate the hCMPs (**E**). The complete hCMP is shown in the larger image (scale bar = 400 μm), while the individual channels and incorporated cells are visible in the inset (scale bar = 50 μm).

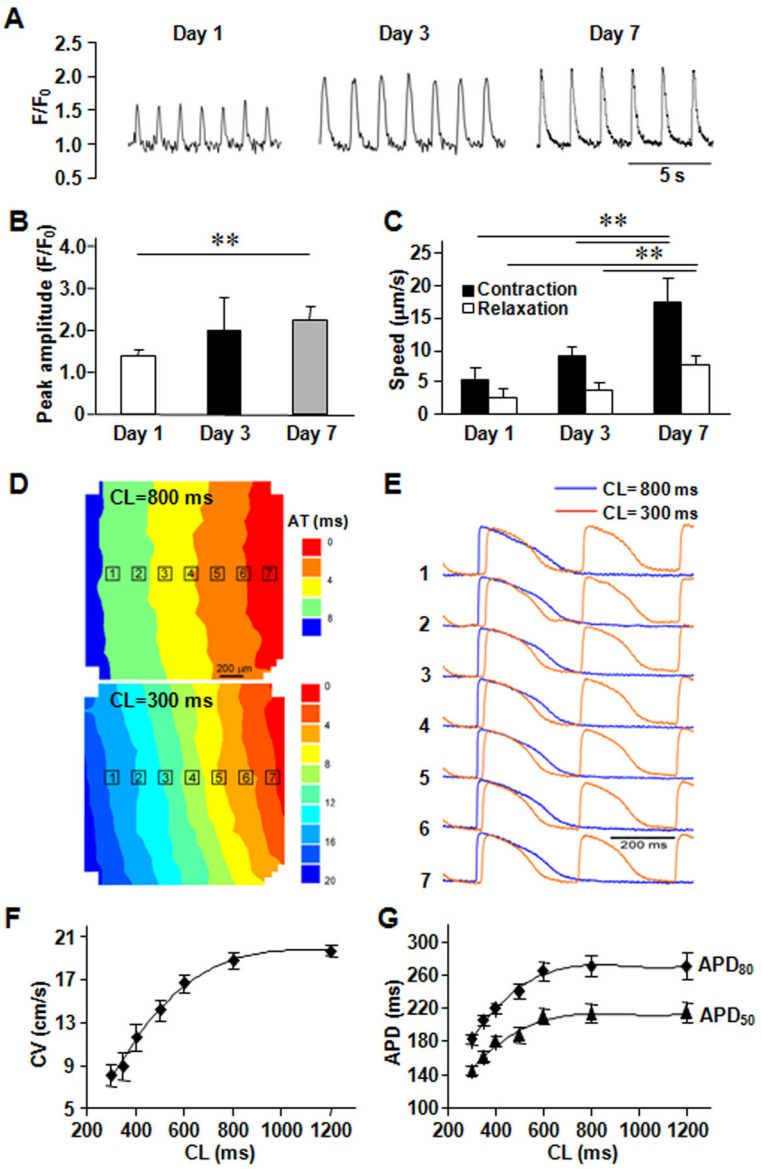

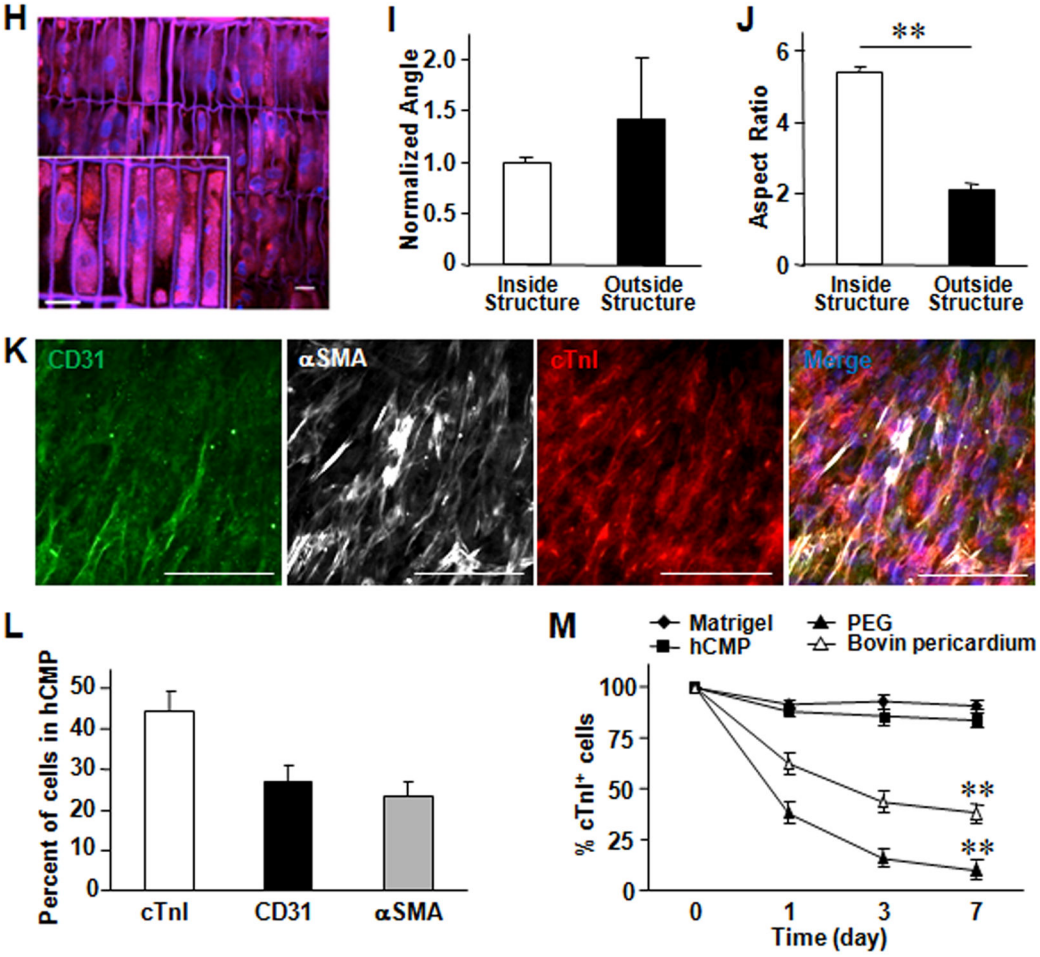


**Figure 2.** ***In vitro*** **assessments of the hCMP**

(**A**) Calcium transients were recorded in hCMPs on day 1, 3, and 7 after cell seeding, and used to calculate the (**B**) peak amplitude ($F/F_0$; n ≥ 50 cells per time point). (**C**) Videos of the beating hCMPs were taken on day 1, 3, and 7 and evaluated with motion vector analysis software to calculate the speeds of contraction and relaxation (n=4 hCMPs per time point). (**D–G**) Action potential propagation in hCMP was measured on day 7 (n=4). (**D**) Representative isochronal map of activation spread and (**E**) selected optical $V_m$ traces recorded during pacing with cycle length (CL) of 800 and 300 ms. AT, activation time; Dependence of **(F)** conduction velocity (CV) and **(G)** action potential duration ($APD_{50}$ and $APD_{80}$) on pacing CL. (**H**) hCMPs were stained with DAPI on day 7; then, autofluorescence images were obtained via 2-photon microscopy (scale bar = 20 μm) and used to calculate the cells' (**I**) angle of alignment relative to the long axis of the engineered channel and (**J**) aspect ratio. (**K**) On day 7, ECs, SMCs, and CMs were identified in the hCMPs via immunofluorescence staining for the presence of CD31, α-smooth-muscle actin (αSMA), and cardiac troponin I (cTnI), respectively; then (**L**) the proportion of each cell type was calculated (5 fields per hCMP and 4 hCMPs). (**M**) Known quantities of hiPSC-CMs were seeded into Matrigel, polyethylene glycol (PEG), decellularized bovine pericardium, or the engineered scaffold and cultured for 7 days; then, the cells were immunofluorescently

stained for cTnI expression, and cell survival was quantified as the ratio of the number of $cTnI^+$ cells observed to the number of seeded cells. $^{**}P<0.01$.

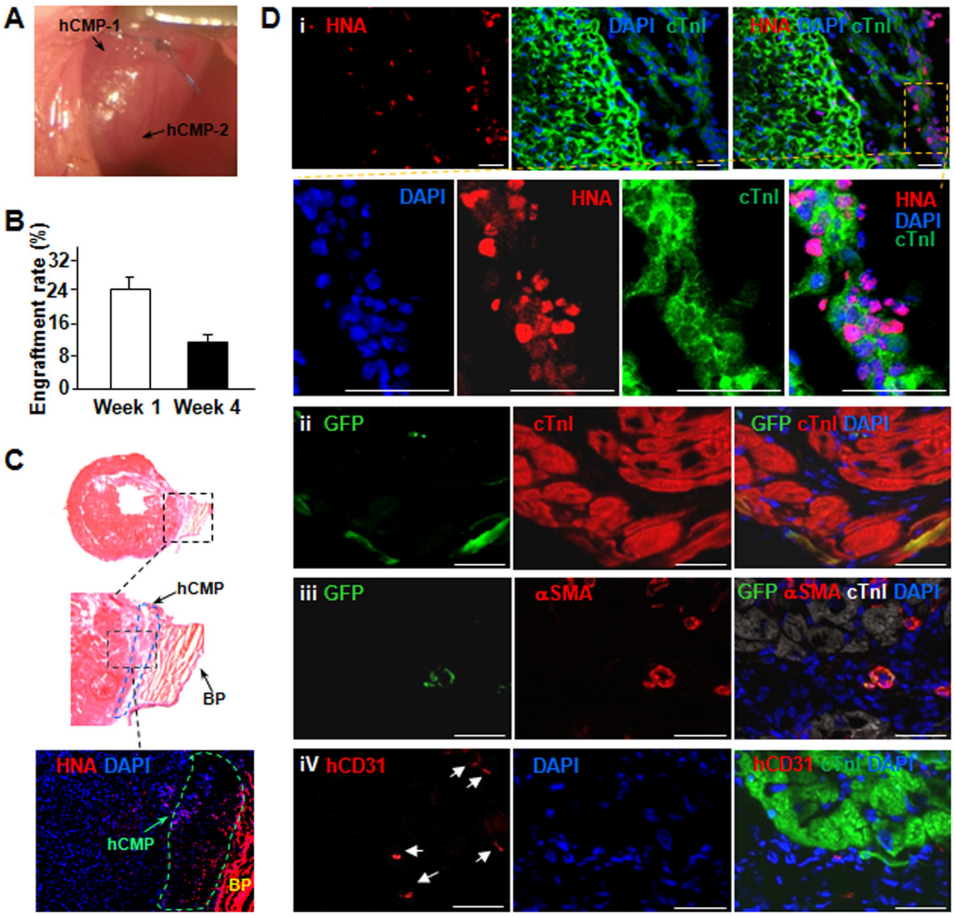


**Figure 3. hCMP engraft and survive after transplantation into the hearts of mice with MI**

Myocardial infarction was surgically induced in mice. Animals in the MI+hCMP group were treated with two hCMPs (0.1 million cells total). (**A**) The representative image showed two transplanted hCMPs on the mouse heart. (**B**) The engraftment rate was determined in animals from the MI+hCMP group at week 1 and 4 after injury via quantitative PCR measurements of the human Y chromosome (n=4 hearts per time point). (**C**) The representative HE staining image and human specific nuclear antigen (HNA) immunostaining image showed engrafted hCMP on the epicardial surface of the heart at week 4 after transplantation. BP=bovine pericardium. (**D**) Sections taken from the region of patch in MI+hCMP animals at week 4 were immufluorescently stained for the presence of HNA, cTnI, green fluorescent protein (GFP), αSMA, and the human isoform of the endothelial marker CD31 (hCD31); nuclei were counterstained with DAPI (scale bar = 50 μm). (**i–ii**) Engrafted hciPSC-CMs were identified by the expression of both HNA and cTnI (**i**) or both GFP and cTnI (**ii**); (**iii**) engrafted hiPSC-SMCs were identified by the expression of both GFP and αSMA; (**iv**) engrafted hiPSC-ECs were identified by the expression of hCD31.

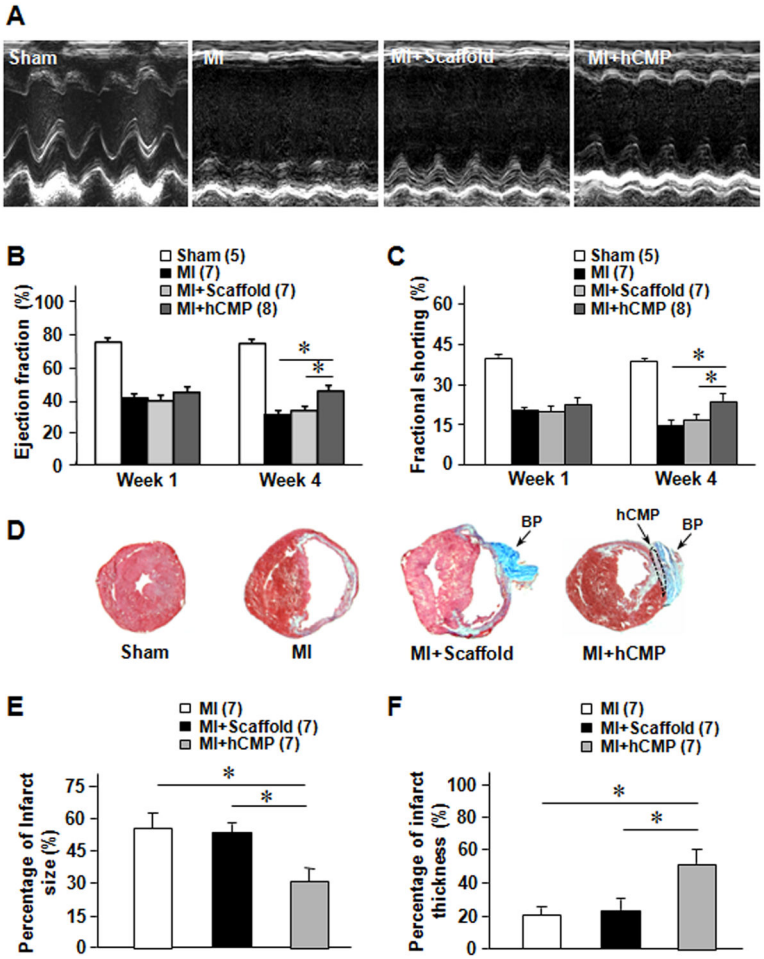


**Figure 4. hCMP transplantation improves cardiac function and reduces infarct size after MI**

(**A–C**) Cardiac function was evaluated at week 1 and 4 via (**A**) echocardiographic assessments of (**B**) left-venticular ejection fraction and (**C**) fractional shortening. (**D–F**) Sections of hearts from animals in different groups were (**D**) Masson's trichrome–stained for histological assessments of (**E**) infarct size and (**F**) infarct wall thickness. Infarct size was calculated as a percentage of the circumflexion length of the left ventricular free wall, and infarct wall thickness was calculated as a percentage of the thickness of the septal wall. *$p$<0.05. BP=bovine pericardium.